HHS Public Access

Author manuscript

Neurogastroenterol Motil. Author manuscript; available in PMC 2020 January 01.

Published in final edited form as:

Neurogastroenterol Motil. 2019 January ; 31(1): e13449. doi:10.1111/nmo.13449.

High resolution optical mapping of gastric slow wave propagation

Hanyu Zhang[1], **Han Yu**[1], **Gregory P. Walcott**[2,1], **Niranchan Paskaranandavadivel**[3,4], **Leo K Cheng**[3,5], **Gregory O'Grady**[3,4], **Jack M. Rogers**[1,*]

[1]Department of Biomedical Engineering, University of Alabama at Birmingham, Birmingham, Alabama, United States [2]Division of Cardiovascular Disease, Department of Medicine, University of Alabama at Birmingham, Birmingham, Alabama, United States [3]Auckland Bioengineering Institute, The University of Auckland, Auckland, New Zealand [4]Department of Surgery, The University of Auckland, Auckland, New Zealand [5]Department of Surgery, Vanderbilt University, Nashville, Tennessee, United States

Abstract

Background: Improved understanding of the details of gastric slow wave propagation could potentially inform new diagnosis and treatment options for stomach motility disorders. Optical mapping has been used extensively in cardiac electrophysiology. Although optical mapping has a number of advantages relative to electrical mapping, optical signals are highly sensitive to motion artifact. We recently introduced a novel cardiac optical mapping method that corrects motion artifact and enables optical mapping to be performed in beating hearts. Here, we reengineer the method as an experimental tool to map gastric slow waves.

Methods: The method was developed and tested in 12 domestic farm pigs. Stomachs were exposed by laparotomy and stained with the voltage-sensitive fluorescence dye di-4-ANEPPS through a catheter placed in the gastroepiploic artery. Fiducial markers for motion tracking were attached to the serosa. The dye was excited by 450 or 505 nm light on alternate frames of an imaging camera running at 300 Hz. Emitted fluorescence was imaged between 607 and 695 nm. The optical slow wave signal was reconstructed using a combination of motion tracking and excitation ratiometry to suppress motion artifact. Optical slow wave signals were compared with simultaneously recorded bipolar electrograms and suction electrode signals, which approximate membrane potential.

Key Results: The morphology of optical slow waves was consistent with previously published microelectrode recordings and simultaneously recorded suction electrode signals. The timing of the optical slow wave signals was consistent with the bipolar electrograms.

*Corresponding author: 1670 University Blvd, Volker Hall B140, Birmingham, AL, 35294, USA, (205) 975-2102, jrogers@uab.edu.

Author Contributions

All authors performed experiments. HZ and HY analyzed data. JMR and HZ wrote the manuscript. NP, LKC, and GOG edited the manuscript.

Conflicts Of Interest

The authors declare no conflicts of interest.

Conclusions & Inferences: Optical mapping of slow wave propagation in the stomach is feasible.

Keywords

electrophysiology; slow wave; motion artifact; optical mapping; slow wave propagation

Introduction

Recently, gastric slow wave propagation has been studied using high-resolution electrical mapping. In this technique, extracellular potentials are recorded from hundreds of electrodes on the stomach's surface.[1, 2] This technology is being used to characterize dysrhythmic slow wave propagation and relate it to motility disorders.[3–6] Detailed understanding of propagation patterns could provide a framework to understand the initiation and maintenance of gastric dysrhythmias.

Optical mapping is an alternative technology for tracking bioelectric waves. It has become a mainstay of experimental cardiac electrophysiology.[7, 8] In optical mapping, tissue is stained with a voltage-sensitive fluorescent dye. Typical dyes shift their excitation and emission spectra to shorter wavelengths in response to depolarization.[9] With appropriate choice of excitation light wavelength and fluorescence emission passband, the intensity of light reaching a photodetector is modulated by membrane potential (V_m).[7, 8]

Optical mapping has several advantages relative to electrical mapping: (1) Smooth muscle repolarization is directly imaged. Repolarization may be a key factor in gastric dysrhythmias as it is in cardiac arrhythmias.[10] While it is possible to detect repolarization in extracellular electrical potentials, this requires careful signal conditioning and postprocessing.[11] (2) Optical mapping signals are not distorted by distant electrical activity or electrical stimuli such as therapeutic pacing. (3) In principle, each camera pixel can produce a distinct V_m signal; thus, optical mapping typically has higher spatial resolution than electrical mapping.

A disadvantage of optical mapping is that optical signals are highly sensitive to motion artifact. In cardiac applications, optical mapping is therefore usually performed in *ex vivo* preparations after pharmacologically arresting muscle contraction.[12] We recently introduced a novel cardiac optical mapping method that corrects motion artifact and enables optical mapping in beating hearts.[13] Here, we reengineer the method for use as an experimental tool to map slow wave propagation in *in vivo* swine stomach.

Methods and Materials

Animal Preparation.

Protocols were approved by the University of Alabama at Birmingham IACUC. We developed the method using 12 farm pigs weighing 25–35 Kg. Animals were anesthetized with atropine/telazol/xylazine (0.04/4.4/4.4 mg kg^{-1}) and maintained with isoflurane. The stomach was exposed by laparotomy. Using a 21-gauge catheter, we cannulated the gastroepiploic artery at mid-corpus. We then infused saline and noted the blanched area. The size of this area varied from preparation-to-preparation, but was on the order of 5×5 cm. To

monitor electrical activity independently of the optical system, we sutured 4 pairs of bipolar electrodes (2-mm silver spheres, ~6 mm separation) around the periphery of the blanched area and connected them to bioamplifiers (BMA-931, CWE, gain 5000, bandpass filter 1–300 Hz). Bipolar electrograms were recorded at 250 Hz. In 5 animals, we also recorded from a suction electrode adjacent to the blanched area (DC-coupled, reference in abdominal cavity), which produced extracellular potentials approximating V_m.[14, 15] Using tissue adhesive, we glued 2-mm-diameter fiducial markers to the blanched region in an unstructured pattern with ~1 cm spacing.

We dissolved the voltage-sensitive dye di-4-ANEPPS (Biotium Inc.) in DMSO (1 mg mL^{-1}) and diluted it in physiological solution to 15 μmol L^{-1}. Sixty mL was slowly injected into the catheter in 10 mL boluses (~1 min each). We occluded the artery distal to the cannula to direct solution into the tissue, repositioning the clamp between boluses to distribute the dye.

Optical Mapping.

We adapted our previous method designed for isolated hearts.[13] Briefly, we used a combination of motion tracking and excitation ratiometry[16] to remove motion artifact. Fluorescence was recorded with a video camera (Andor iXon DV860, 128×128 resolution, 300 Hz, 6 mm focal length ¼” format f/1.0 lens, ~15 cm working distance). Fiducial marker motion in the image plane was tracked as previously described.[13] Linear interpolation within each triangle of markers was used to find the motion of any tissue site within a triangle. The fluorescence emitted from each tissue site was then collected from the locus of pixels that imaged the site as it moved across the image plane.

This scheme removes motion artifact resulting from nonuniform staining and spatial differences in electrical activity. However, new artifact is caused by spatial heterogeneity of excitation light intensity. To eliminate this, we switched the excitation wavelength between 450 nm (blue) and 505 nm (cyan) with each camera frame and selected an emission filter passband of 651±44 nm. In this spectral design, blue-elicited fluorescence is insensitive to smooth muscle V_m, but cyan-elicited fluorescence is inversely modulated by V_m. Motion artifact is common to both signals (which are temporally interlaced when recorded) and is canceled by taking the ratio of blue- to cyan-elicited fluorescence emitted by a tissue site (excitation ratiometry[16]). Our previous publication contains details and analysis.[13]

Excitation light was generated by light-emitting diodes (LED) driven by custom-made electronics. For effective artifact correction, the ratio of the intensity of the excitation light colors must be uniform across the mapped region. To achieve this, we used LEDs designed for color mixing (Luxeon C, Lumileds). We soldered LEDs to custom aluminum-core circuit boards with 4 LED pads. Each pad had 2 blue and 2 cyan LEDs arranged in a close-packed checkerboard pattern. Boards were housed in color-mixing wells machined from white acetyl plastic covered with a shortpass filter (B-410, Hoya) and holographic diffusing sheets (90% transmission 40° angle, Edmund Optics). Four such units were mounted on a custom-made cooling water jacket and positioned in a ring around the camera’s lens. We adjusted LED drive current so that the intensities of each wavelength were equal. The optical mapping instrumentation is shown in the supporting material (S1).

Data Acquisition.

To keep the stomach warm and moist, we irrigated it with warm saline and covered the incision with plastic sheeting and warming packs except during acquisition runs. Data acquisition duration was 60 s. The camera's shutter signal was recorded synchronously with the electrograms to temporally align optical and electrical recordings. To reduce large-scale motion, we paused the ventilator (with lungs filled) during recording. Typically, 1–2 complete slow waves were captured in each recording.

Results

Figure 1A illustrates V_m reconstruction. The top two panels are deinterlaced blue- and cyan-elicited fluorescence signals recorded from a single pixel. In this anesthetized, fasted preparation, slow waves (frequency ~2–3 min^{-1}) induce small, non-functional contractions. Motion artifact nevertheless swamps out V_m, and blue- and cyan-elicited signals have similar morphology, even though they have markedly different V_m sensitivity. The next two panels show the blue- and cyan-elicited signals after motion tracking: artifact is greatly attenuated, but still present. Applying ratiometry recovers a signal (5^{th} panel) morphologically consistent with microelectrode recordings from gastric smooth muscle cells (e.g., ref. 17). Figure 1B shows suction electrode and optical V_m signals that were recorded simultaneously from adjacent sites in a different animal. The V_m deflections—in particular their durations—are consistent with one another.

We were able to acquire V_m signals from an area spanning at least 3 marker triangles in 7 animals. In 2 of these animals, staining was sufficient to map wave propagation across the majority of the mapped region. Figure 2 is an example from one animal. Panels A and B show that deflection timing in optical signals is consistent with bipolar electrograms recorded from sites on the periphery of the optically mapped region. Figure 2D maps slow wave activation times. Propagation is right-to-left (proximal-to-distal) with velocity ~1cm s^{-1}, which is consistent with electrical mapping data in the pig.[18] Activation together with recovery are animated in Video S2. Video S3 shows propagation in the second animal.

Discussion

To our knowledge, this is the first demonstration of *in vivo* optical mapping of gastric slow wave propagation. Because the V_m-sensitive fluorescence signal is small compared to motion artifact, attenuating this artifact is essential. Here, we used a combination of motion tracking and excitation ratiometry adapted from methods we developed for cardiac mapping.[13]

With our staining method, the area with satisfactory fluorescence was highly variable. Stomach staining is complicated by collateral circulation that can rapidly wash out dye. Improving staining technique to consistently enable mapping over a larger region will be important in further development of the method. This might be achieved by infusing dye at the celiac trunk, possibly by using an isolated stomach preparation[19] or endovascular delivery in *in situ* preparations. In this study, depolarization could be reliably identified, but repolarization, which is more gradual, was observable, but much less distinct. Improved

staining, or possibly the use of long-wavelength dyes optimized for blood-perfused preparations,[20] may amplify V_m relative to residual artifact and noise and sharpen repolarization localization. Another limitation is large rigid-body motion (e.g., respiration) that moves the mapped region out of frame or out of focus. In the present study, we paused the ventilator while recording. It might also be possible to mechanically isolate the stomach from respiratory motion, or to gate breaths between slow waves. This would not be an issue in an isolated preparation.

We conclude that optical mapping of gastric slow wave propagation is feasible. With continued development, the method has the potential to improve understanding of normal and dysrhythmic gastric electrical function, eventually leading to better diagnosis and treatment of gastric motility disorders.

Supplementary Material

Refer to Web version on PubMed Central for supplementary material.

Acknowledgements

This work was supported by funding from the Health Research Council of New Zealand and NIH grant R01HL115108. The authors thank Shannon Salter and Sharon Melnick for their expert assistance with animal management.

Abbreviations

V_m	Membrane potential
LED	Light emitting diode
CCD	Charge coupled device

References

1. O'Grady G,Angeli TR and Lammers WJEP. The Principles and Practice of Gastrointestinal High-Resolution Electrical Mapping In: Cheng LK, Pullan AJ and Farrugia G, eds. New Advances in Gastrointestinal Motility Research Dordrecht: Springer Netherlands; 2013: 51–69.
2. Cheng LK, Du P and O'Grady G. Mapping and Modeling Gastrointestinal Bioelectricity: From Engineering Bench to Bedside. Physiology. 2013;28:310–317. [PubMed: 23997190]
3. Angeli TR, Cheng LK, Du P, Wang TH-H, Bernard CE, Vannucchi M-G, Faussone-Pellegrini MS, Lahr C, Vather R, Windsor JA, Farrugia G, Abell TL and O'Grady G. Loss of Interstitial Cells of Cajal and Patterns of Gastric Dysrhythmia in Patients with Chronic Unexplained Nausea and Vomiting. Gastroenterology. 2015;149:56–66.e5. [PubMed: 25863217]
4. O'Grady G, Angeli TR, Du P, Lahr C, Lammers WJ, Windsor JA, Abell TL, Farrugia G, Pullan AJ and Cheng LK. Abnormal initiation and conduction of slow-wave activity in gastroparesis, defined by high-resolution electrical mapping. Gastroenterology. 2012;143:589–598 e3. [PubMed: 22643349]
5. Lammers WJ, Ver Donck L, Stephen B, Smets D and Schuurkes JA. Focal activities and re-entrant propagations as mechanisms of gastric tachyarrhythmias. Gastroenterology. 2008;135:1601–11. [PubMed: 18713627]
6. Sanders KM, Kito Y, Hwang SJ and Ward SM. Regulation of Gastrointestinal Smooth Muscle Function by Interstitial Cells. Physiology (Bethesda). 2016;31:316–26. [PubMed: 27488743]

7. Efimov IR, Nikolski VP and Salama G. Optical imaging of the heart. Circ Res. 2004;95:21–33. [PubMed: 15242982]
8. Herron TJ, Lee P and Jalife J. Optical imaging of voltage and calcium in cardiac cells & tissues. Circ Res. 2012;110:609–23. [PubMed: 22343556]
9. Loew LM. Design and Use of Organic Voltage Sensitive Dyes. Advances in experimental medicine and biology. 2015;859:27–53. [PubMed: 26238048]
10. Antzelevitch C and Burashnikov A. Overview of Basic Mechanisms of Cardiac Arrhythmia. Cardiac electrophysiology clinics. 2011;3:23–45. [PubMed: 21892379]
11. Paskaranandavadivel NN, Cheng LK, Du P, Rogers JM and O'Grady G. High-resolution mapping of gastric slow wave recovery profiles: biophysical model, methodology and demonstration of applications. American journal of physiology Gastrointestinal and liver physiology. 2017:ajpgi 00127 2017.
12. Fedorov V, Lozinsky I, Sosunov E, Anyukhovsky E, Rosen M, Balke C and Efimov IR. Application of blebbistatin as an excitation-contraction uncoupler for electrophysiologic study of rat and rabbit hearts. Heart Rhythm. 2007;4:619–626. [PubMed: 17467631]
13. Zhang H, Iijima K, Huang J, Walcott GP and Rogers JM. Optical mapping of membrane potential and epicardial deformation in beating hearts. Biophys J. 2016;111:438–451. [PubMed: 27463145]
14. Angeli TR, Du P, Paskaranandavadivel N, Janssen PW, Beyder A, Lentle RG, Bissett IP, Cheng LK and O'Grady G. The bioelectrical basis and validity of gastrointestinal extracellular slow wave recordings. J Physiol. 2013;591:4567–79. [PubMed: 23713030]
15. Bortoff A Configuration of intestinal slow waves obtained by monopolar recording techniques. Am J Physiol. 1967;213:157–62. [PubMed: 6027912]
16. Bachtel AD, Gray RA, Stohlman JB, Bourgeois EB, Pollard AE and Rogers JM. A novel approach to dual excitation ratiometric optical mapping of cardiac action potentials with DI-4-ANEPPS using pulsed LED excitation. IEEE Trans Biomed Eng. 2011;58:2120–2126. [PubMed: 21536528]
17. Sanders KM, Ward SM and Koh SD. Interstitial Cells: Regulators of Smooth Muscle Function. Physiol Rev. 2014;94:859–907. [PubMed: 24987007]
18. Egbuji JU, O'grady G, Du P, Cheng LK, Lammers WJEP, Windsor JA and Pullan AJ. Origin, propagation and regional characteristics of porcine gastric slow wave activity determined by high-resolution mapping. Neurogastroenterology & Motility. 2010;22:e292–e300. [PubMed: 20618830]
19. Salvati P and Whittle BJ. Investigation of the vascular actions of arachidonate lipoxygenase and cyclo-oxygenase products on the isolated perfused stomach of rat and rabbit. Prostaglandins. 1981;22:141–56. [PubMed: 6794098]
20. Matiukas A, Mitrea BG, Qin M, Pertsov AM, Shvedko AG, Warren MD, Zaitsev AV, Wuskell JP, Wei MD, Watras J and Loew LM. Near-infrared voltage-sensitive fluorescent dyes optimized for optical mapping in blood-perfused myocardium. Heart Rhythm. 2007;4:1441–51. [PubMed: 17954405]
21. Efimov IR, Huang DT, Rendt JM and Salama G. Optical mapping of repolarization and refractoriness from intact hearts. Circulation. 1994;90:1469–80. [PubMed: 8087954]

Key Points

- Current gastric slow wave mapping technology uses arrays of extracellular electrodes. Optical mapping is a complementary technology that is widely used in the heart. Here, we investigate its feasibility in the stomach.
- Membrane potential signals can be imaged across the surface of the *in vivo* pig stomach using voltage-sensitive fluorescent dye in combination with techniques to correct motion artifact.
- High resolution imaging of slow wave propagation has the potential to improve understanding of normal and dysrhythmic gastric electrical function.

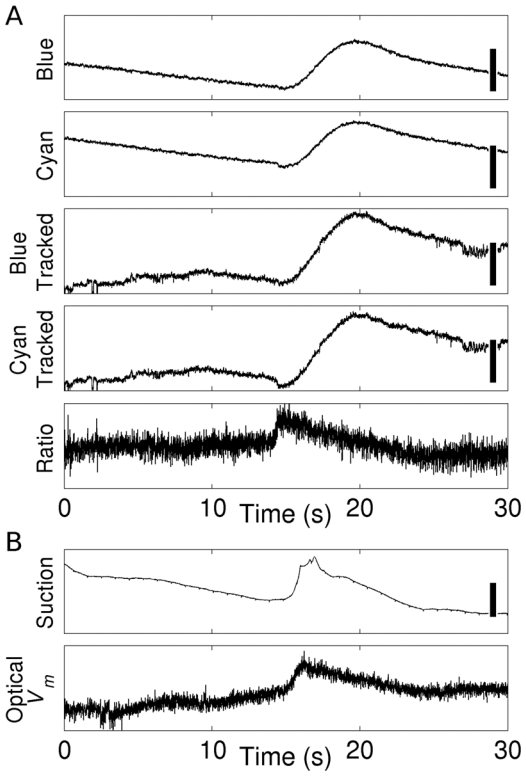

Figure 1.

Reconstruction of optical V_m signals. A, Motion artifact correction. Blue/Cyan: deinterlaced blue- and cyan-elicited fluorescence signals before motion tracking. Calibration bars represent 100 CCD counts. Blue Tracked/Cyan Tracked: deinterlaced blue- and cyan-elicited fluorescence signals after motion tracking. Calibration bars represent 50 CCD counts. Ratio: ratio of the Blue Tracked to Cyan Tracked signals, which is proportional to V_m. B, Comparison of a suction electrode signal, which approximates V_m, and an optical V_m signal simultaneously recorded from a site ~2 cm away. The scale bar in the suction electrode signal is 200 μV. Data in A and B are from different animals.

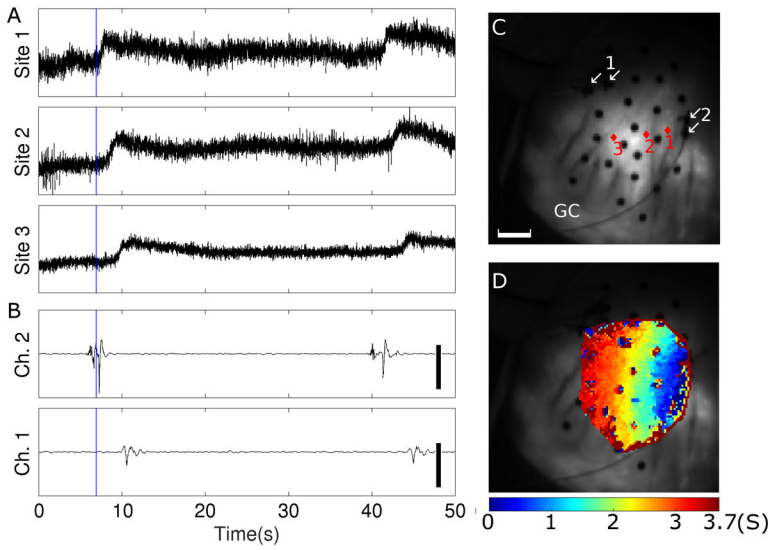

Figure 2.

Optical mapping of slow wave propagation. A, Reconstructed optical slow wave signals. B, Bipolar electrical recordings. Scale bars are 600 μV. C, Fluorescence image of the marked region. Black circles are fiducial markers. Red diamonds show optical recording sites from Panel A. White arrows show the locations of the two electrodes in each bipolar recording site from Panel B. The scale bar is 10 mm. GC indicates the greater curvature. D, Isochronal map showing propagation of the 1st slow wave in A and B. Colors indicate time of steepest V_m upstroke (i.e., electrical activation). Activation and recovery for this wave are animated in Supporting Video S2. The blue line in panels A and B indicates time 0 for the isochronal map in panel D. The area of the mapped region is not constant, but is ~10 cm^2 and contains ~2600 pixels spaced by ~0.6 mm in each direction. An optical V_m signal was generated for each pixel that was within the mapped region in the first frame of the recording. Effective spatial resolution was reduced to ~1.5 mm in each direction by a 5-pixel moving-average spatial filter (von Neumann neighborhood with r=1) that was applied before finding activation times.